Mon. Not. R. Astron. Soc. **332,** 714–722 (2002)

Short-period line profile and light variations in the Be star λ Eridani

L. A. Balona[1]★ and D. J. James[2, 3]
[1]*South African Astronomical Observatory, PO Box 9, Observatory 7935, Cape Town, South Africa*
[2]*School of Physics and Astronomy, University of St Andrews, St Andrews, Fife KY16 9SS*
[3]*Observatoire de Genève, Chemin des Maillettes, no 51, CH-1290 Sauverny, Switzerland*

Accepted 2002 January 15. Received 2002 January 14; in original form 2001 September 4

ABSTRACT

We present three seasons of photometric observations and one season of intensive high-dispersion spectroscopic observations of the Be star λ Eridani. We show that only one period, $P = 0.70173$ d, is present in the photometry, although there are large light amplitude variations from season to season. We confirm a suspicion that light outbursts repeat at intervals of about 475 d. A total of 348 echelle spectra of the star were obtained over a 2-week observing run. We show that the periodic variations are present in the emission wings of the helium lines, in the emission wings of the Hα line and in the absorption cores of Hβ and Hγ. Together with the fact that the periodic variations appear outside the projected rotational velocity limit, this indicates that they are associated with circumstellar material immediately above the photosphere and supports the idea of corotating gas clouds. We present evidence in support of a true rotational period of $2P = 1.40346$ d and suggest that the mass loss in Be stars is caused by centrifugal magnetic acceleration.

Key words: line: profiles – stars: early-type – stars: emission-line, Be – stars: individual: λ Eri.

1 INTRODUCTION

Historically, the periodic variations in Be stars have been interpreted as being non-radial pulsation (NRP). The circumstellar material responsible for Balmer line emission in Be stars arises from the photosphere, and it has also been suggested that NRP is the mass loss mechanism (see, e.g., Baade 2000). However, we know that the period of the light and line profile variations are not significantly different from the expected period of rotation (Balona 1995). An alternative interpretation is that the periodic variations are a result of circumstellar material corotating with the star. Indeed, since the origin of the circumstellar material arises from localized outbursts on the stellar photosphere (even in the NRP interpretation), one may well expect a rotational variation of some kind.

It is with these ideas in mind that we decided to re-observe a number of Be stars more intensively than in the past. The aim of the project was to obtain enough data to discriminate between NRP and the rotational hypothesis by means of prolonged, intensive high-resolution spectroscopic and photometric observations of a few objects. The following Be stars have been observed: η Cen (Balona 1999), ω CMa (Balona, Aerts & Štefl 1999), ζ Tau (Balona & Kaye 1999), ϵ Cap (Balona & Lawson 2001), μ Cen (Balona et al. 2001a) and ω Ori (Balona et al. 2001b). In these stars we find that the periodic variations are present in the emission lines and in the photospheric absorption lines, indicating that the source of the variation extends to the circumstellar material.

In this paper we continue the series of observations of bright Be stars. λ Eri (HR 1679, HD 33328, B2 IVne) was one of the first stars in which short-period variations were discovered. Bolton (1981) found a period of 0.701 538 d ($f = 1.42544$ cycle d^{-1}) from radial velocities obtained during 1971 and 1980 and photometry obtained in 1977. Antonello, Mantegazza & Pastori (1984) obtained some radial velocities and photometry but were unable to reproduce the 0.70-d period. Percy (1986) obtained photometric observations over several seasons. He was able to confirm that the data are consistent with the 0.70-d period, but the sampling was not suited to an independent period analysis. Balona et al. (1987) obtained intensive photometry and were able to show that the most probable period does, indeed, correspond to $P = 0.70$ d. This was later confirmed by Balona, Cuypers & Marang (1992) who found $P = 0.70165$ d. Mennickent, Sterken & Vogt (1998) analysed photometry of λ Eri and suggested that light outbursts may recur at intervals of about 470 d.

The first intensive high-resolution spectroscopic observations of λ Eri were made by Smith (1989) from which a period $P = 0.70165$ d was found. He found no correlation between the amplitude of the line profile variations and the level of Hα emission (however, see Kambe et al. 1993). The line profile variations of He I λ6678 could be described by two NRP modes with $\ell = 2$ ($P = 0.70$ d) and $\ell = 8$. The period of the $\ell = 8$ mode was found to be variable, but between 0.28 and 0.33 d. A proper period analysis

★E-mail: lab@saao.ac.za

was, however, not conducted. Different types of spectral transients were found and classified and interpreted in terms of small-scale magnetic flaring. Correlations of far-ultraviolet (far-UV) flux variations and transients in the He I λ6678 line profile were discussed by Smith & Polidan (1993). A model in which the condensation of high-density structures at some elevation over the star is proposed to account for these observations. The He I λ6678 line in Be stars generally shows emission wings whenever Hα emission is present. Smith et al. (1994) find that this emission can be used as a sensitive monitor of localized hotspots on the surface of the star. Smith et al. (1996) find that transients are also visible in several other optical He I lines and not only in the λ6678 line. In further investigations of transient features in the helium line profiles of λ Eri, Smith et al. (1997a) simulated He I line emission from model slabs suspended above the star. They find that Lyman-pumped recombination in a slab of high density may explain the results.

A very interesting and important result was the discovery of a giant X-ray flare in λ Eri (Smith et al. 1993). As with most B-type stars, λ Eri is a soft X-ray emitter, but the X-ray intensity increased by a factor of 6 over a period of 39 h. The brightening can be fitted to a Raymond–Smith temperature of 14×10^6 K. They conclude that the flare most probably originated in the star itself. Smith et al. (1997b) monitored the star simultaneously in X-ray, far-UV and ground-based observations during a week in 1995. Mild X-ray flux variations were followed by a sinusoidal decay in the far-UV flux with a 3-h period. At the same time an increase in Hα emission was observed.

2 OBSERVATIONS

Spectroscopic observations at SAAO were obtained using the GIRAFFE echelle fibre-fed spectrograph attached to the Cassegrain focus of the 1.9-m telescope. The GIRAFFE spectrograph has a resolving power of about 32 000. The 1024×1024 TEK charge-coupled device CCD chip gives a dispersion of 0.06–0.09 Å pixel^{-1}. A Th–Ar arc lamp was used for wavelength calibration, with arc spectra being taken at regular intervals to calibrate possible drifts. Flat fielding was accomplished by illuminating the camera with uniform light using a tungsten filament lamp and a diffusing screen. The blaze correction was determined by measuring the response across each order when the fibre was illuminated by a tungsten lamp. The wavelength range was 4400–6680 Å spread over 45 orders. Exposure times were normally 10 min for a signal-to-noise (S/N) ratio of 150–200. A total of 348 spectra of λ Eri was obtained (see Table 1) over a consecutive 2-week period in 2000 (31 October–13 November).

In order to study the line profile variations, the continuum needs to be determined. Placing the continuum by hand is not an easy process. We preferred to rectify the spectra with the aid of a synthetic spectrum calculated using the SPECTRUM code (Gray & Corbally 1994). To do this, we calculated a synthetic spectrum covering the full echelle wavelength range using a Kurucz solar-abundance model atmosphere appropriate to a B2 IV star and broadened with $v\sin i = 194$ km s^{-1}. To rectify the spectrum, each echelle order was divided by the synthetic spectrum and the result fitted with a third-order polynomial. A direct comparison of the rectified spectra with the synthetic spectrum showed that the above procedure is quick and effective.

Photometry was obtained using the modular photometer attached to the 0.5-m reflector of SAAO, Sutherland simultaneously with the echelle data at the same site. We used all four Strömgren *uvby* filters and the two local comparison stars, HR 1640 and HR 1748. All three stars were observed in sequence through a light neutral density filter. The unpublished observations were made in 1994, 2000 and 2001. In Table 2 we present a log of all observations suitable for period analysis of the star. For some data sets, only *b*-band data are available, so the period analysis will be confined to this band. The data were reduced to a uniform system using the following mean values for the comparison stars: HR 1640: $y = 6.422$, $b = 6.340$, $v = 6.348$, $u = 6.543$, HR 1748: $y = 6.347$, $b = 6.323$, $v = 6.373$, $u = 6.586$.

Table 1. Observing log for the spectroscopy. The Julian day, with respect to JD 245 1800, is shown for the first and last spectrum of λ Eri on the given night. *N* is the number of spectra obtained on that night.

Start	End	*N*
49.39	49.63	30
50.39	50.63	32
51.39	51.62	30
52.39	52.62	31
53.38	53.62	28
54.38	54.59	28
55.44	55.58	9
56.55	56.63	10
57.38	57.62	32
58.37	58.63	33
59.37	59.63	34
60.37	60.50	18
62.37	62.62	33

Table 2. Strömgren *b* photometry of λ Eri obtained at SAAO and ESO. The year, source, mean value of *b* and number of data points are given. The last column is the amplitude of the periodic component at $P = 0.702$ d.

JD	Year	Source	$\langle b \rangle$	*N*	Amplitude
244 6415	1985A	SAAO[a]	4.216	315	5.7 ± 1.1
244 6379	1985B	ESO[a]	4.211	64	3.9 ± 2.3
244 6415	1985C	SAAO[a]	4.209	63	6.7 ± 2.4
244 6774	1986	SAAO[a]	4.223	344	3.4 ± 0.4
244 7109	1987	SAAO[b]	4.167	38	16.0 ± 3.5
244 7182	1988	SAAO[b]	4.212	200	5.1 ± 0.6
244 7181	1988	ESO[b]	4.214	113	5.2 ± 0.7
244 9679	1994	SAAO	4.177	125	6.5 ± 0.8
245 1856	2000	SAAO	4.150	62	21.8 ± 1.9
245 1918	2001	SAAO	4.203	83	3.3 ± 1.2

[a]Balona et al. (1987);
[b]Balona et al. (1992).

3 ROTATIONAL VELOCITY

We assume that the mean line profile of a large number of spectra is the best estimate of the photospheric line profile. In Figs 1 and 2 we show mean profiles of all measured lines.

The projected rotational velocity of λ Eri was measured by Slettebak (1982) to be 220 km s^{-1}. More recently, Ballereau, Chauville & Zorec (1995) found $v \sin i = 275$ km s^{-1} by modelling the He I λ4471 line. We determined $v \sin i$ from various helium and metal lines using the intrinsic line profile calculated from the SPECTRUM program and a non-linear least-squares optimizing

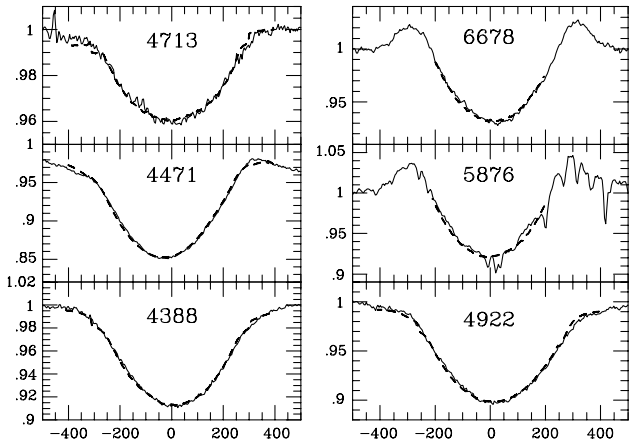

Figure 1. Mean rectified profiles of the helium lines (solid line) and the best model fit to the projected rotational velocity (dashed line). The range over which the fit was performed is the range covered by the dashed line. The abscissa is in units of km s^{-1} as measured from the laboratory wavelength of the line.

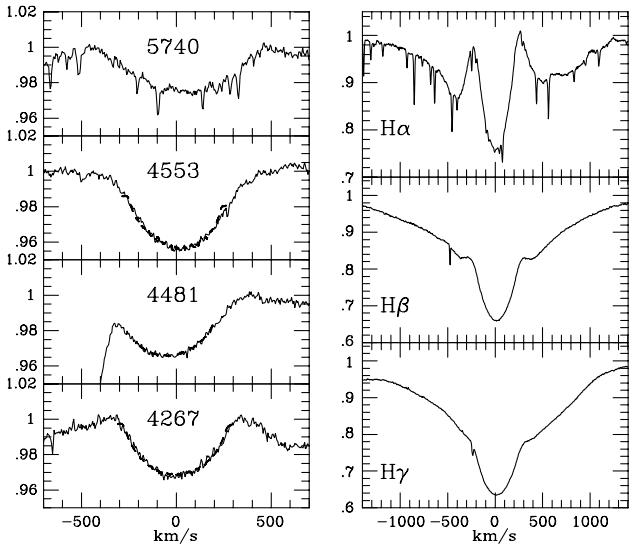

Figure 2. Mean rectified profiles of C II λ4267, Mg II λ4481 and Si III λλ4553, 5740 and the hydrogen lines. The dashed line is the best fit for the projected rotational velocity, as in Fig. 1.

algorithm, leaving the radial velocity as a free parameter. For lines showing emission, we fitted only the core of the line profiles. Results are given in Table 3 and the fits are shown in Fig. 1. In some Be stars, the helium lines give significantly lower values than the metal lines, but this is not the case in λ Eri. From all helium lines we obtain $v \sin i = 257 \pm 9$ km s^{-1} and from the metal lines we find $v \sin i = 252 \pm 8$.

The radial velocity of the Mg II λ4481 line is very much lower than the others, but this is probably to the severe blending with the neighbouring He I λ4471 line and only part of the line could be used. The spread in the radial velocities of the helium lines is quite large (the standard deviation is 7 km s^{-1}), and none of the velocities are significantly different from the mean ($\langle V_r \rangle = 14.4 \pm 2.9$).

The *Hipparcos* parallax of λ Eri is 1.86 ± 0.88 mas. The uncertainty is too large to give a useful parallax which would be helpful in determining the radius. For a B2 star, Balona (1995) obtains $R/R_\odot = 4.8$, 6.6 and 8.4 for classes V, IV and III, respectively. Porter (1996) finds a polar radius of $5.4\,R/R_\odot$, $M/M_\odot = 9.6$ and $V_{\rm crit} = 477$ km s^{-1} for a B2 dwarf. Assuming $R/R_\odot = 7 \pm 3$ and taking the equatorial rotational velocity to be $v_{\rm eq} = 250$ km s^{-1}, the longest rotational period is $P = 1.4 \pm 0.6$ d. The uncertainty in the stellar radius is always a major problem in estimating the probable period of rotation.

Table 3. Projected rotational velocity, $v \sin i$ (km s^{-1}) obtained by non-linear least-squares fitting for various lines (laboratory wavelengths given). The standard deviation of the fit, σ, is in continuum units. For the helium lines, the range of fit was −300 to +300 km s^{-1}, while for the other lines it was −150 to +210 km s^{-1}. The column labelled RV is the radial velocity of the line (km s^{-1}) as obtained from the fit. The last column is the equivalent width in Å.

Line	$v \sin i$	σ	RV	EW
He I λ4387.929	250	0.0013	8.2	0.58
He I λ4471.682	257	0.0015	7.8	1.08
He I λ4713.376	261	0.0016	17.4	0.29
He I λ4921.931	241	0.0016	26.8	0.76
He I λ5875.966	235	0.0076	14.0	0.27
He I λ6678.151	298	0.0017	12.0	0.35
All He lines	257 ± 9			
C II λ4267.167	267	0.0017	3.3	0.21
Mg II λ4481.228	245	0.0010	−32.4	0.28
Si III λ4552.622	243	0.0018	5.0	0.34
All metal lines	252 ± 8			

4 THE PERIOD: PHOTOMETRY

In Fig. 3 we show the periodograms of the unpublished data sets, 1994, 2000 and 2001. We analysed these data for periodicities up to a frequency of 20 cycle d^{-1}. The 1994 data set shows a clear periodicity at $f = 1.42$ cycle d^{-1} and an amplitude of 7 mmag. No further periods are present. The 2000 data are ambiguous; the frequency could be 1.50 cycle d^{-1} or its 1 cycle d^{-1} aliases at $f = 0.5$ or 2.5 cycle d^{-1}. There is another closely spaced peak at $f = 1.34$ cycle d^{-1} and its aliases. Both peaks have quite large amplitudes of 17 and 15 mmag; no further significant periods are present. The 2001 data do not show anything very significant. Analyses of the combined 2000 and 2001 data show nothing significant apart from the $P = 0.70$-d period. This demonstrates that the two close peaks found in 2000 cannot be coherent multiperiodicities.

One of the peculiar characteristics of Be stars is that an approximately sinusoidal light curve might develop a secondary minimum that subsequently deepens to give a double-wave variation (Balona, Sterken & Manfroid 1991). A double-wave variation will not be easily detected in a typical periodogram which assumes that the underlying variation is sinusoidal. The peculiarity of the periodogram for 2000 prompted us to investigate this possibility. In Fig. 4 we show the y light curve phased with $P = 0.70173$ d and the double period $2P = 1.40346$ d (the other passbands show the same behaviour). The figure shows that $P = 0.70173$ d certainly fits the data, but also that the double period may be an even better fit. However, the phase coverage is not complete enough to make a definite statement in this regard. The double peak in the 2000 periodogram is simply a mathematical representation of a non-sinusoidal variation and cannot be taken as

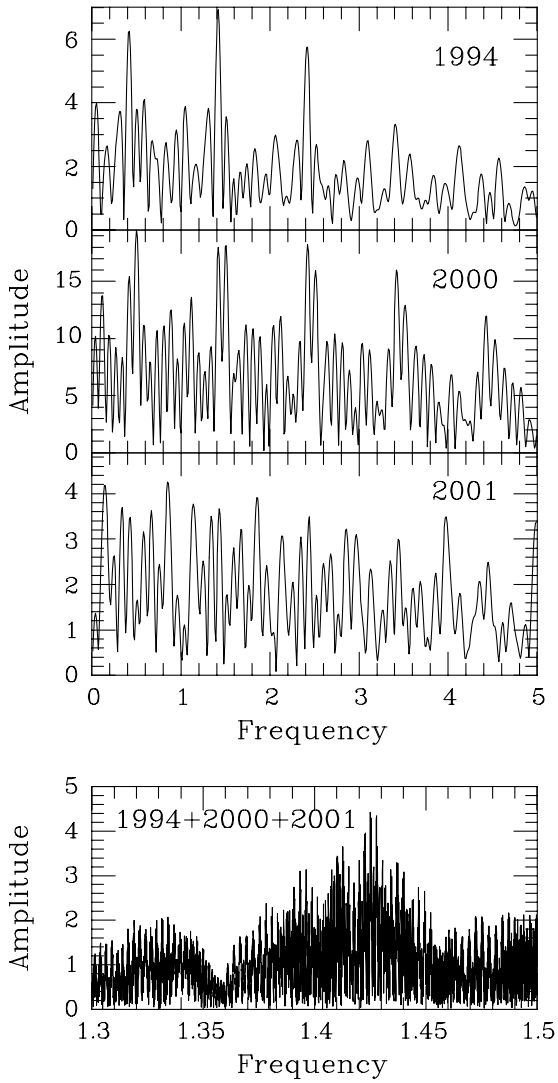

Figure 3. Fourier periodograms of Strömgren *b* photometry of λ Eri obtained at SAAO. From top to bottom the panels show the periodograms of the 1994, 2000 and 2001 data. The bottom panel shows the periodogram of all three data sets combined. The frequency is in cycle d^{-1} and the amplitude in millimag.

evidence for coherent multiperiodicity because these peaks disappear when the data from 2001 are included.

The difference in the periodograms from season to season is quite typical of Be stars since they are active on all time-scales. Nevertheless, an underlying period is usually present. If such a coherent period is present at all times, it should be visible in the periodogram of the combined data. If there is more than one coherent period over this time, the additional periodicities should also be visible in the combined data. To determine the most probable period, we removed the mean from each data set and performed a periodogram analysis on the combined data sets of Table 2 (1395 Strömgren *b* observations). The result is that only a single period is present over this time interval, and we can confidently conclude that there are no further significant periods. We find $f = 1.42504 \pm 0.00002$ cycle d^{-1}, corresponding to $P = 0.70173 \pm 0.00001$ d, which is essentially the same period as found by Bolton (1981) from the radial velocities. In Fig. 5 we show the mean Strömgren *b* light curve from all the data shown in Table 2. The mean amplitude is 4.5 mmag.

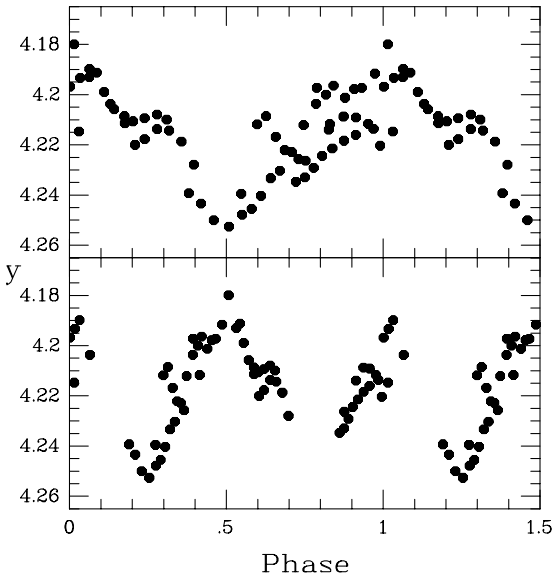

Figure 4. The Strömgren-*y* light curve of λ Eri during 2000 November phased with $P = 0.70173$ d (top panel) and with $2P = 1.40346$ d (bottom panel).

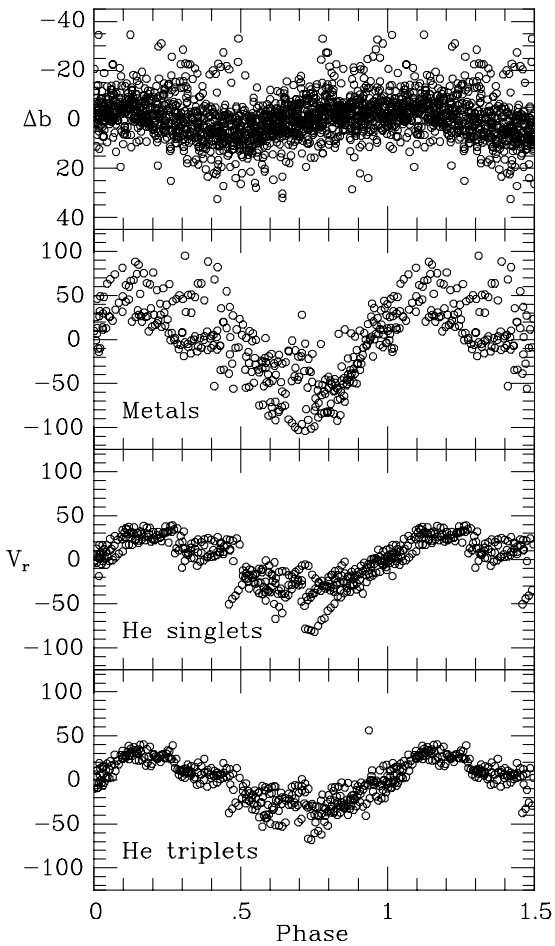

Figure 5. Top panel: the Strömgren *b* light curve of λ Eri phased with $P = 0.70173$ d using the combined data sets of Table 2. The other panels show the radial velocities (measured from maximum absorption) of the He triplets, singlets and metal lines phased with the same period for the 2000 season. In all cases the epoch of phase zero is HJD 245 1800.058 (maximum light).

Table 4. Amplitudes and phase differences with respect to the *b*-band of the $P = 0.702$-d period for three seasons. Amplitudes are in millimagnitudes and phases are given as fraction of the period.

Band	Amplitude	$\phi - \phi_b$
1994:		
u	10.2 ± 3.4	−0.118 ± 0.06
v	6.1 ± 0.8	−0.030 ± 0.02
b	6.5 ± 0.8	0.000 ± 0.02
y	6.1 ± 0.6	−0.001 ± 0.02
2000:		
u	25.7 ± 2.3	−0.013 ± 0.01
v	23.1 ± 2.3	0.004 ± 0.01
b	21.8 ± 1.9	0.000 ± 0.01
y	20.4 ± 2.0	−0.008 ± 0.01
2001:		
u	4.4 ± 1.3	−0.012 ± 0.05
v	3.1 ± 1.2	−0.035 ± 0.06
b	3.3 ± 1.1	0.000 ± 0.06
y	4.0 ± 1.0	−0.064 ± 0.04

Table 2 shows the amplitude for each season. There appears to be a trend for higher amplitudes to coincide with higher brightness. The sudden increase in brightness and amplitude during 1987 and 2000 is particularly interesting. Mennickent et al. (1998) have suggested that λ Eri undergoes episodes of sudden brightening, followed by rapid fading, with a period of about 470 ± 9 d. The brightening episodes in 1987 and 2000 fit their ephemeris quite well, especially if the period is slightly revised to 475 d. They attribute these brightening events as being the formation and dissipation of a circumstellar envelope. These episodes appear to coincide with temporary Hα emission, which we also observe during the 2000 maximum.

For some seasons, four-colour Strömgren *uvby* photometry was obtained. In Table 4 we show the amplitudes of all four colours and the phase differences relative to the *b* band. There is a slight decrease in amplitude for longer wavelengths, but no significant phase differences.

5 THE PERIOD: RADIAL VELOCITIES

The precise meaning of the term 'radial velocity' has been discussed in other papers of this series. We use it to refer to the displacement of the point of maximum absorption relative to the laboratory wavelength. The centroid of the absorption profile can also be used, but the variation is less pronounced. Also, there is considerable subjectivity in deciding how much of the wings to include in calculating the centroid, particularly if wing emission is present. To determine the core velocity from the point of maximum absorption requires smoothing and the results depend to some extent on the degree of smoothing. Moreover, the presence of small-scale absorption features travelling across the line profile causes discontinuities. On the other hand, the results are independent of wing emission.

We calculated the radial velocity from maximum core absorption as well as from the centroid. We decided to exclude wing emission. In every case the periodograms of individual lines showed maximum power at the photometric frequency. No significant periodicity is left when a fit with this period is removed from the data. This is demonstrated in Fig. 6 which shows the periodograms of the core radial velocities of the helium singlets, triplets and metal lines on the left and the corresponding periodograms after removal of the photometric period on the right. In Table 5 we show the radial velocity amplitudes. The amplitude of the metal lines is significantly larger than that of the helium lines owing mostly to the very high amplitude of the Mg II λ4481 line. This line suffers from severe blending and the result may not be very trustworthy. In Fig. 5 we show the mean radial velocity curve (from maximum absorption) for the helium singlets (λλ4388, 4922, 6678), helium triplets (λλ4471, 5876 and 4713) and metal lines (λλ4481, 4553). The metal lines have a significantly higher amplitude. As expected, the core absorption radial velocity amplitude is significantly higher than the centroid amplitude.

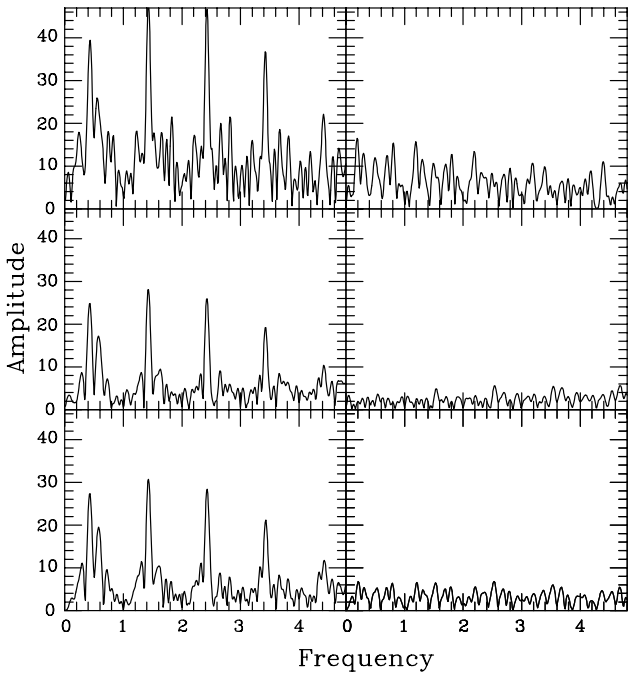

Figure 6. Left-hand panels: periodograms of the radial velocities of the helium singlet (bottom panel), helium triplet (middle panel) and metal lines (top panel). Right-hand panels: the corresponding periodograms after removing a Fourier fit with the photometric period $P = 0.70173$ d.

Table 5. For each spectral line listed in the first column, the radial velocity amplitude from the position of maximum absorption, A_{RV}, and from the centroid, A_{cen}, is listed. Units are km s^{-1}.

Line	A_{RV}	A_{cen}
C II λ4267.167	35.5 ± 1.9	49.6 ± 2.5
He I λ4387.929	43.6 ± 1.2	8.3 ± 0.4
He I λ4471.682	35.5 ± 1.9	15.0 ± 0.3
Mg II λ4481.228	57.7 ± 2.5	8.3 ± 0.6
Si III λ4552.622	37.2 ± 3.1	53.5 ± 3.2
He I λ4713.376	39.9 ± 2.0	20.4 ± 0.8
He I λ4921.931	33.8 ± 0.8	14.0 ± 0.4
He I λ5875.966	13.1 ± 1.0	26.1 ± 0.6
He I λ6678.151	18.8 ± 1.8	24.3 ± 0.8
He singlets	31.7 ± 1.0	15.4 ± 0.4
He triplets	29.3 ± 1.0	19.1 ± 0.4
Metals	49.5 ± 2.1	30.9 ± 1.7

Apart from the photometric period, there is no evidence for any other period in the helium lines. Our conclusion is that the spectroscopic period is the same as the photometric period, which has been stable for over a decade and that the star has only one period, $P = 0.70173$ d.

6 LINE PROFILE VARIATIONS

The radial velocities only give information concerning the core of the line profile. To obtain a complete picture of the line profile variations, one needs to study the variations over the whole profile. The most convenient way of doing this is to construct 'difference profiles' by dividing each line profile by the mean line profile. In this way, even small departures from the mean line profile can be visualized in a grey-scale diagram. By stacking difference spectra as a function of time in a grey-scale image, the variation of the line profiles as a function of time can be easily seen.

In Figs 7 and 8 we show stacked grey-scale spectra for a number of lines during one night. It is clear that the variations are practically the same in all lines, in spite of the difference in level where the lines are formed. The variations are prominent in the emission wings of He I λλ6678 and 5876. Variations in the cores of the hydrogen lines have been seen in other Be stars, but they are particularly prominent in λ Eri, even in the core of Hα.

We note from Figs 7 and 8 that the profile variations extend beyond $v \sin i = 255\,\mathrm{km\,s^{-1}}$. Variations as far as $\pm 300\,\mathrm{km\,s^{-1}}$ from line centre are seen. We also note that the variations shown in Fig. 7 are far from the simple 'barber pole' diagrams typical of non-radial pulsation (see, for example, Schrijvers & Telting 1999). The excess absorption feature is actually composed of two close strands. Moreover, there is a weak absorption feature on the red side of the line, which appears to move from red to blue. This starts on the extreme red wing at phase 0.4 and joins the main absorption feature at phase 1.2. The feature is clearly seen in all six helium lines as a Y-shaped fork extending from phase 1.2. The feature is quite clearly seen in Fig. 8 as well.

In Fig. 9 we show the mean line profile of He I λ6678 phased in 20 bins with $P = 0.70173$ d. It is evident that the wing emission strength varies. A phase dispersion minimization periodogram analysis of blue-wing emission strength shows that the most probable period is twice the photometric period, $2P = 1.40346$ d, but there is not a big difference between P and $2P$ for red-wing emission strength. In Fig. 10 we show the height above the continuum of the blue and red emission wings and also a radial velocity trace of the absorption subfeature for He I λ6678 phased with $2P$. In Fig. 11 we show the same thing for Hα. Both figures show almost identical variations. When the emission intensity is maximum in the blue wing, it is minimum in the red wing and vice versa. The variation in blue- and red-wing intensities appears to have two periodic components, as the phase minimization periodogram indicates. One component is a smooth variation with period $2P$ on which is superimposed a secondary, sharper, minimum at phase 0.3. The double-wave periodicity is particularly clear in the blue wing of He I λ6678.

One explanation for the variability of the emission-line strength in the wings of He I λ6678 is that it is a result of the underlying variability of the absorption-line component. We could suppose that the emission component is in fact constant, but that it is the radial velocity movement of the underlying absorption-line component that periodically reduces the emission strength of the

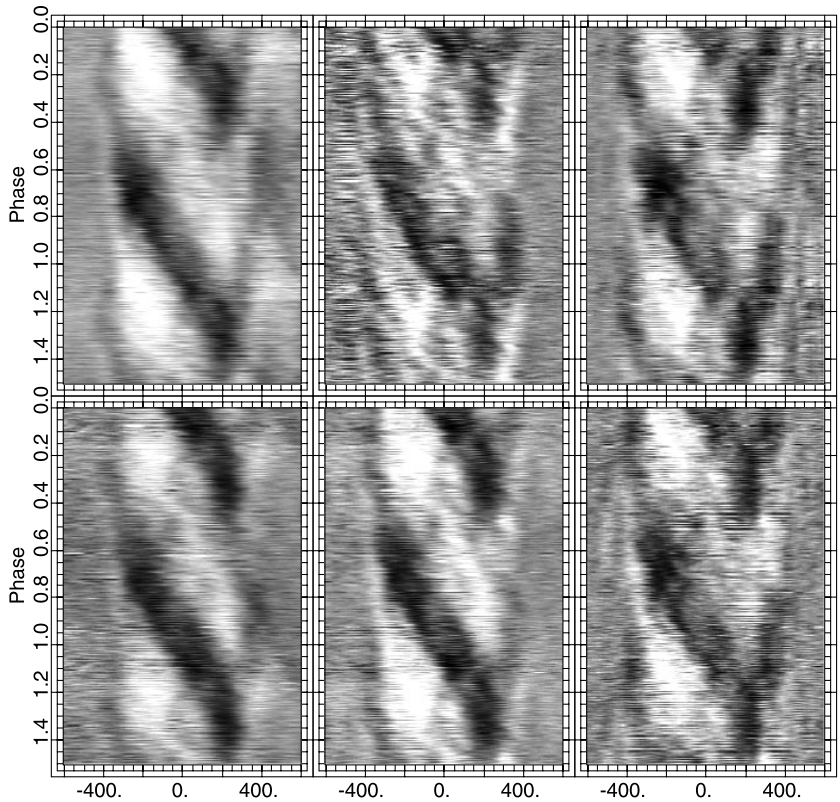

Figure 7. Grey-scale difference spectra of helium lines phased with $P = 0.70173$ d. The displacement from the centre of the line profile is expressed in km s^{-1}; the epoch of phase zero if HJD 245 1800.058 which corresponds to maximum light. Bottom panels, left to right: He I λλ4388, 4922, 6678. Top panels, left to right: He I λλ4471, 4713, 5876.

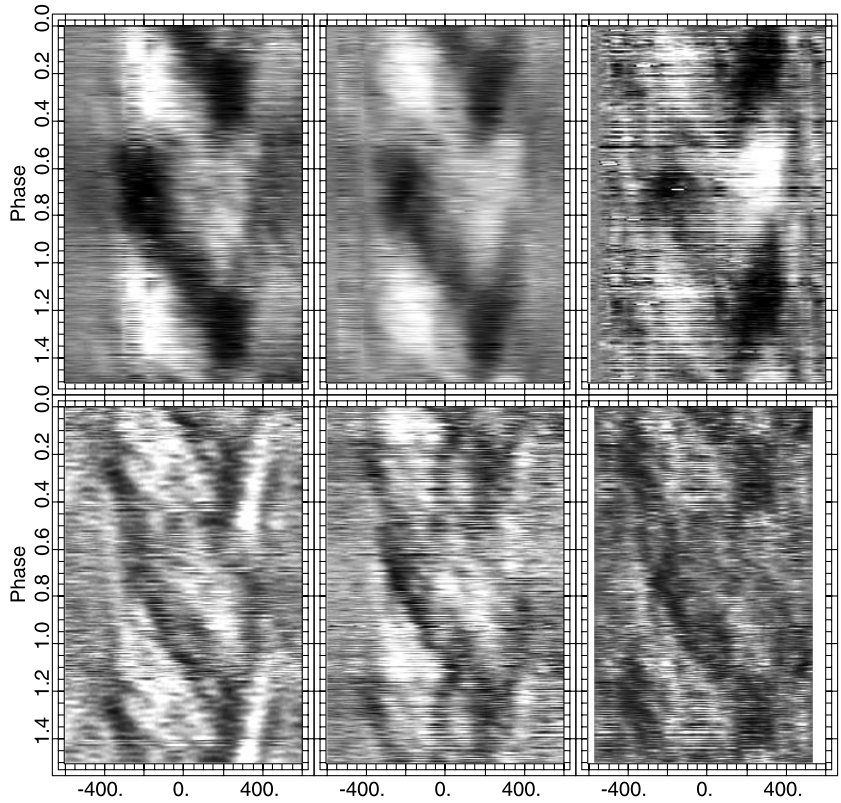

Figure 8. The same as in Fig. 7 but for some metal and hydrogen lines. Bottom panels, left to right: C II λ4267, Si III λ4553, Si III λ5740. Top panels, left to right: Hγ, Hβ, Hα.

red and blue wings. We note, first of all, that the absorption component has much the same line broadening as the other, pure absorption, helium lines (Table 3). Considering the strength of wing emission, one would have thought that the absorption intensity in the wings of He I λ6678 would have been considerably reduced, leading to a smaller $v\sin i$. This is clearly not the case, suggesting that we are seeing practically all the photospheric component of the line profile and that the emission wings are a separate, circumstellar, component rotating at higher velocity. Furthermore, note that at certain phases wing emission almost completely disappears (Fig. 9). To do this would require the underlying absorption component intensity to be comparable to the emission component intensity at the same wavelength in the extreme line wings. This could only happen if the true absorption component were to be much broader than other helium lines. Finally, the radial velocity amplitude of the core of He I λ6678 is only $19\,\mathrm{km\,s^{-1}}$ (Table 5) – much too small to account for the supposed movement of the line, which would have to be of the order of $100\,\mathrm{km\,s^{-1}}$, the typical width of the emission wings. We can conclude confidently that the variation in wing emission is a result of the variability of the circumstellar disc and not the photosphere.

The equivalent widths (EW) of some lines also vary, but there is no evidence for a preference of $2P$ over P. He I λ4388 shows the largest EW amplitude. In Fig. 12 we show the EW variations of the He I lines $\lambda\lambda$4388, 4922 and 4713 phased with $2P$. The EWs of all three lines vary in phase, reaching a maximum when the residual absorption feature is near the stellar meridian. At this phase, the Hα and He I λ6678 blue emission wing has maximum intensity and the red emission wing minimum intensity.

Although the $P = 0.702$-d period (or perhaps the $2P$ period suggested by the emission-line intensity variations) is well established and coherent over many years, it is clear that there are large and rapid changes in amplitude from season to season. Moreover, the variations are by no means exactly repeatable from cycle to cycle. There are changes in intensity and detailed structure of the absorption subfeature that are difficult to quantify. The structure of the absorption subfeature is itself complex, appearing to consist of two close strands of residual absorption moving from blue to red. The spectral line transients reported by Smith et al. (1996) appear to be random variations in the detailed structure of the residual absorption bands and must be seen in this context rather than specific localized features.

7 CONCLUSION

In this series of papers, we have presented the most intensive spectroscopic observations of individual Be stars to date. In every star we find that the periodic variation is present in lines showing emission wings, particularly in the He I λ6678 line. In the shell star ϵ Cap, where all helium line profiles are strongly distorted by circumstellar emission, the periodic variations are easily visible (Balona & Lawson 2001). In λ Eri, ϵ Cap, μ Cen (Balona et al. 2001a) and ω Ori (Balona et al. 2001b) periodic variations are also visible in the core of Hα, Hβ and Hγ. It follows that the periodic variations are associated with circumstellar material, though they also affect the photospheric metal lines. In μ Cen an extra residual absorption feature that moves from red to blue is seen at non-periodic intervals. In all of these stars, only one period is present and this period is indistinguishable from the period of rotation of the star. The line profile variations, though periodic, are very complex. In η Cen, a highly complex structure repeats in a period

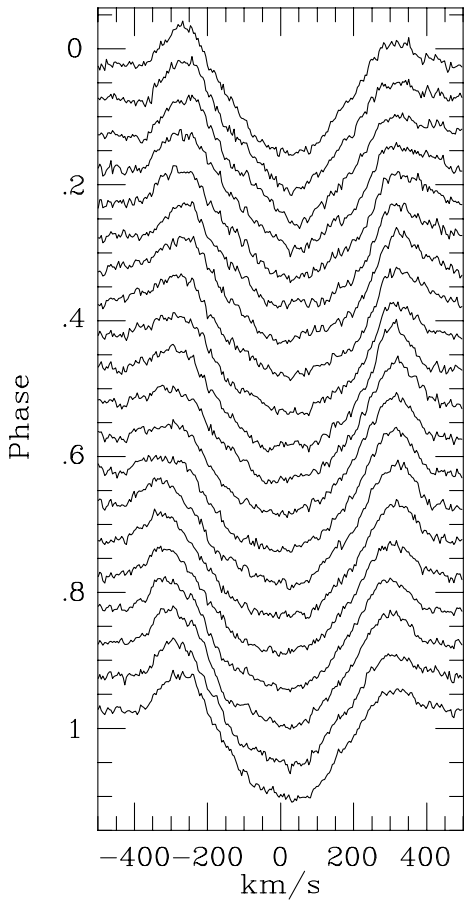

Figure 9. Line profiles of He I λ6678 phased with $P = 0.70173$ d. The epoch of phase zero, HJD 245 1800.058, coincides with maximum light. Note that the strength of the emission wings varies with the same period.

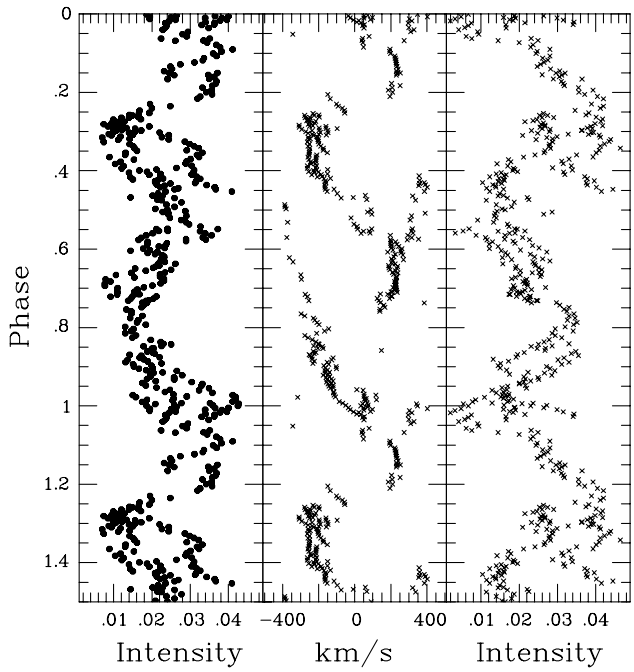

Figure 10. The height above the continuum of the blue (left-hand panel) and red (right-hand panel) emission wings of He I λ6678 phased with $P = 1.40346$ d. The middle panel shows the radial velocity of the absorption subfeature phased with the same period. The epoch of phase zero is HJD 245 1800.058.

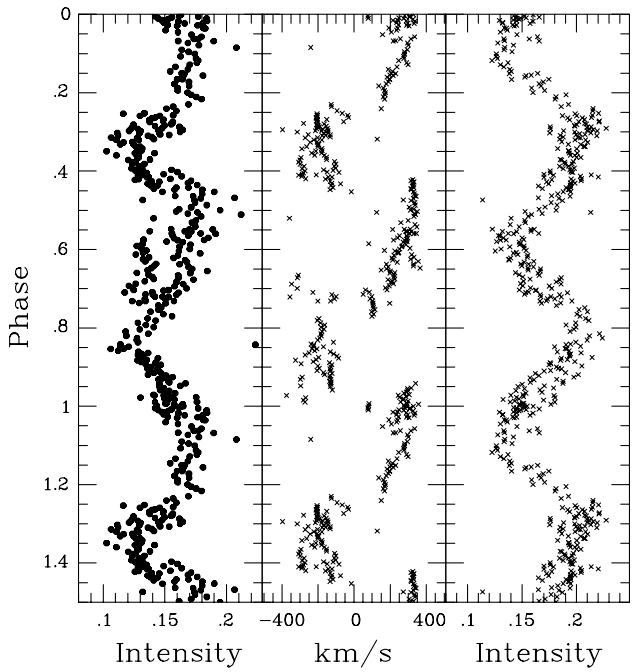

Figure 11. The same as in Fig. 10 but for Hα.

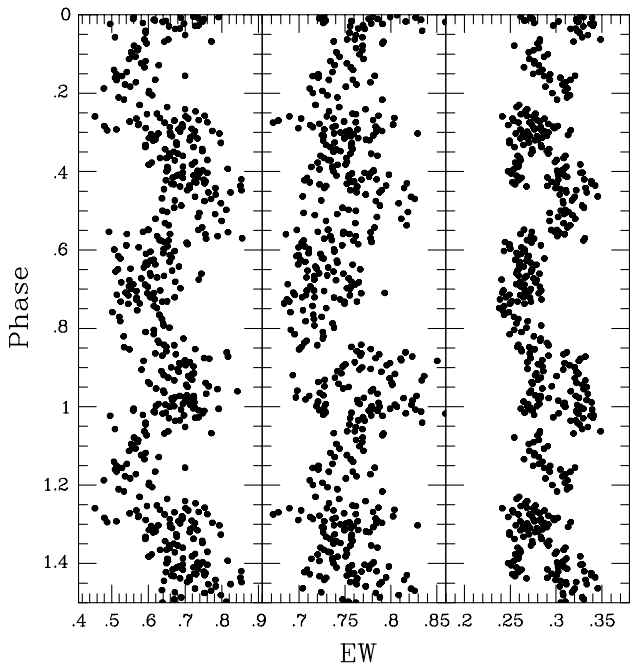

Figure 12. The equivalent width variation (in angstrom) of three He I lines: λ4388 (left), λ4922 (middle) and λ4713 (right) phased with $P = 1.40346$ d. The epoch of phase zero is HJD 245 1800.058.

equivalent to the period of rotation and alternate residual absorption and emission is seen at the wings.

The complexity of the line profile variations is mirrored by the light variations that occur on all time-scales. It is well known, for example, that an approximately sinusoidal light curve might develop a secondary minimum that subsequently deepens to give a double-wave variation (Balona 1991) in the next season. It is therefore important to check for a possible double-wave periodicity in all Be stars. In μ Cen, for instance, the spectroscopy clearly

indicates a period of about 0.5 d, but there is no light amplitude at this period, only at twice the spectroscopic period of 1.0 d (Balona et al. 2001a). Previous work on this star (Rivinius et al. 2001), which indicated multiperiodicity, is not confirmed in the more intensive data coverage of Balona et al. (2001a). There is some indication from the variation of the emission-line strength, as well as the light curve in the 2000 season, that the true period in λ Eri might also be a double-wave one.

For many years it has been supposed that the periodic variations are a result of non-radial pulsation (NRP), though it is acknowledged that some other mechanism must be responsible for the random fluctuations that are seen in the line profiles and light variations. We argue that it is extremely unlikely, given the active nature of these stars, that some form of rotational modulation is not seen. We know that outbursts occur at localized places on or near the photosphere (Balona 1999), and this must lead to rotational modulation, even if the initial outburst was initiated by NRP. We have suggested that NRP is not required to explain the periodic variations and, indeed, cannot account for the non-periodic, random, occurrence of a counter-moving absorption subfeature in μ Cen (Balona et al. 2001), nor the fact that the period of light variation is twice the supposed pulsational period.

In this paper we have argued that the periodic variability of wing emission in He I λ6678 must be caused by variability in the circumstellar material and not the photosphere. This is, in general, true in the other Be stars that we have observed. For example, in ζ Tau (Balona & Kaye 1999) the helium line that displays periodic variability has a classic shell profile which is impossible to model by line formation in the photosphere. In ϵ Cap (Balona & Lawson 2001), which is a shell star, all the helium lines are severely distorted by the circumstellar medium even at the line centre, yet all undergo the same periodic line profile variations. It is difficult to understand how NRP can affect the immediate circumstellar environment so as to cause strong periodic modulations of the emission wing intensities. In this star we also note that the line profile variations appear to extend well outside the rotational velocity limit, which can only be understood if the variation is caused by circumstellar material. The presence of periodic variations in the circumstellar material and the fact that the period of variation is indistinguishable from the rotational period of the star (Balona 1990, 1995) shows that we need to consider the possibility of corotating structures as the mechanism causing the periodic variations. A weak magnetic field in a rapidly rotating star can be an efficient driving mechanism for mass loss (Belcher & MacGregor 1976) and offers a natural explanation for corotating gas clouds and the outbursts seen in Be stars (Balona 2000).

We note from Fig. 7 that at some phases two absorption subfeatures are visible on opposite limbs. In terms of the magnetic rotator model, such a situation can only arise if the true rotation period is $P_{\rm rot} = 2P = 1.40346$ d and if we assume two diametrically placed residual absorption centres. We saw in Section 3 that the longest rotational period is $P = 1.4 \pm 0.6$ d. Hummel & Vrancken (2000) estimate an angle of inclination $i = 57°$ from the shape of the Hα profile. Assuming $v \sin i = 255\,{\rm km\,s^{-1}}$ we obtain an equatorial rotational velocity $v_{\rm e} = 311\,{\rm km\,s^{-1}}$ and $R = 8.6\,{\rm R}_\odot$. This is consistent with the best estimate of $R/{\rm R}_\odot = 7 \pm 3$ discussed in Section 3. Adopting an effective temperature $T_{\rm eff} = 24\,000$ K (Mennickent et al. 1998) gives $\log L/{\rm L}_\odot = 4.345$ or $M_V = -3.75$, which is typical for a B2 giant or subgiant. The expected parallax is about 2.6 mas, which is consistent with the *Hipparcos* value of 1.86 ± 0.88 mas.

If, on the other hand, the rotational period is taken to be $P_{\rm rot} = P = 0.702$ d, the radius will be half as large, $R \approx 4.3\,{\rm R}_\odot$, leading to $M_V = -2.25$, which is compatible with the spectral type if the star is close to the ZAMS. However, the expected parallax of 5.1 mas is 3.7 standard deviations higher than the *Hipparcos* value. We conclude that not only is $P_{\rm rot} = 2P$ consistent with all available data, but that $P_{\rm rot} = P$ is improbable because it should have given a much larger parallax than is observed.

ACKNOWLEDGMENTS

DJJ thanks the British Particle Physics and Astronomy Research Council for a post-doctoral research fellowship, and the Royal Society for a European research grant. DJJ would like to acknowledge the continued positive influences of Mrs J. Pryer.

REFERENCES

Antonello E., Mantegazza L., Pastori L., 1984, Ap&SS, 104, 245
Baade D., 2000, in Smith M. A., Huib H., Fabregat J., eds, ASP Conf. Ser. Vol. 214, Proc. IAU Colloq. 175, The Be Phenomenon in Early-Type Stars. Astron. Soc. Pac., San Franciso, p. 178
Ballereau D., Chauville J., Zorec J., 1995, A&AS, 111, 423
Balona L. A., 1990, MNRAS, 245, 92
Balona L. A., 1995, MNRAS, 277, 1547
Balona L. A., 1999, MNRAS, 306, 407
Balona L. A., 2000, in Smith M. A., Huib H., Fabregat J., eds, ASP Conf. Ser. Vol. 214, Proc. IAU Colloq. 175, The Be Phenomenon in Early-Type Stars. Astron. Soc. Pac., San Franciso, p. 1
Balona L. A., Kaye A. B., 1999, ApJ, 521, 407
Balona L. A., Lawson W. A., 2001, MNRAS, 321, 131
Balona L. A., Marang F., Monderen P., Reitermann A., Zickgraf F.-J., 1987, A&AS, 71, 11
Balona L. A., Sterken C., Manfroid J., 1991, MNRAS, 252, 93
Balona L. A., Cuypers J., Marang F., 1992, A&AS, 92, 533
Balona L. A., Aerts C., Štefl S., 1999, MNRAS, 305, 519
Balona L. A., James D. J., Lawson W. A., Shobbrook R. R., 2001a, MNRAS, 324, 1041
Balona L. A., Aerts C., Božić H., Guinan E. F., Handler G., James D. J., Kaye A. B., Shobbrook R. R., 2001b, MNRAS, 327, 1288
Belcher J., MacGregor K. B., 1976, ApJ, 210, 498
Bolton C. T., 1981, in Jaschek M., Groth C., eds, Proc. IAU Symp. 98, Be Stars. Reidel, Dordrecht, p. 181
Gray R. O., Corbally C. J., 1994, AJ, 107, 742
Hummel W., Vrancken M., 2000, A&A, 359, 1075
Kambe E., Ando H., Hirata R., Walker G. A. H., Kennelly E. J., Matthews J. M., 1993, PASP, 105, 1222
Mennickent R. E., Sterken C., Vogt N., 1998, A&A, 330, 631
Percy J. R., 1986, PASP, 98, 342
Porter J. M., 1996, MNRAS, 280, L31
Rivinius Th., Baade D., Štefl S., Townsend R. H. D., Stahl O., Wolf B., Kaufer A., 2001, A&A, 369, 1058
Schrijvers C., Telting J. H., 1999, A&A, 342, 453
Slettebak A., 1982, ApJS, 50, 55
Smith M. A., 1989, ApJS, 71, 357
Smith M. A., Polidan R. S., 1993, ApJ, 408, 323
Smith M. A., Grady C. A., Peters G. J., Feigelson E. D., 1993, ApJ, 409, L49
Smith M. A., Hubeny I., Lanz T., Meylan T., 1994, ApJ, 432, 392
Smith M. A., Plett K., Johns-Krull C. M., Basri G. S., Thomson J. R., Aufdenberg J. P., 1996, ApJ, 469, 336
Smith M. A., Cohen D. H., Hubeny I., Plett K., Basri G., Johns-Krull C. M., MacFarlane J. J., Hirata R., 1997a, ApJ, 481, 467
Smith M. A., Murakami T., Ezuka H., Anandarao B. G., Chakraborty A., Corcoran M. F., Hirata R., 1997b, ApJ, 481, 479

This paper has been typeset from a TEX/LATEX file prepared by the author.